PLANT ECOLOGY

Global climatic drivers of leaf size

Ian J. Wright,[1]* Ning Dong,[1,2] Vincent Maire,[1,3] I. Colin Prentice,[1,4] Mark Westoby,[1] Sandra Díaz,[5] Rachael V. Gallagher,[1] Bonnie F. Jacobs,[6] Robert Kooyman,[1] Elizabeth A. Law,[1,7] Michelle R. Leishman,[1] Ülo Niinemets,[8] Peter B. Reich,[9,10] Lawren Sack,[11] Rafael Villar,[12] Han Wang,[1,13] Peter Wilf[14]

Leaf size varies by over a 100,000-fold among species worldwide. Although 19th-century plant geographers noted that the wet tropics harbor plants with exceptionally large leaves, the latitudinal gradient of leaf size has not been well quantified nor the key climatic drivers convincingly identified. Here, we characterize worldwide patterns in leaf size. Large-leaved species predominate in wet, hot, sunny environments; small-leaved species typify hot, sunny environments only in arid conditions; small leaves are also found in high latitudes and elevations. By modeling the balance of leaf energy inputs and outputs, we show that daytime and nighttime leaf-to-air temperature differences are key to geographic gradients in leaf size. This knowledge can enrich "next-generation" vegetation models in which leaf temperature and water use during photosynthesis play key roles.

Leaf temperature is a key control on plant metabolic rates. Photosynthetic carboxylation increases strongly with temperature, but so too do catabolic processes such as dark respiration and photorespiration (*1*). Thus, net photosynthetic rate tends to peak at intermediate temperatures, with the optimum temperature typically higher in species from warmer regions (*2*, *3*). Very high or low temperatures can impair enzyme function, disrupt membranes and cellular processes, and if sufficiently extreme, cause irreparable tissue damage (*1*). Plants show a variety of adaptations for increasing the proportion of the day that leaves can operate in near-optimal temperature ranges for photosynthesis and for avoiding temperature extremes (*4*, *5*). Pendulous leaves with reflective leaf surfaces may avoid high midday temperatures (*6*), for example, whereas clumped canopy arrangements in alpine plants help to avoid extreme cold (*7*). Nonetheless, the most conspicuously varying trait that affects leaf temperature is the size of individual leaves.

Across the plant kingdom, leaves vary from less than 1 mm^2 to greater than 1 m^2 in area (*8*). Larger leaves have a thicker boundary layer that slows sensible heat exchange with the surrounding air, meaning that—all else equal—they develop larger leaf-to-air temperature differences than that of smaller leaves (*9*, *10*). All leaves are cooled by transpirational water loss, but this is particularly critical for large leaves, which face greater risk of potentially serious heat damage at high air temperatures and high irradiance, especially when soil water is limiting (*2*). These principles are central to well-known theories for optimal leaf size based on daytime leaf energy budgets (*2*, *9*, *11*–*14*), which predict disadvantages to being large-leaved at hotter, drier, and high-irradiance sites. In support of these predictions, many studies have shown smaller mean leaf sizes at sites with lower mean annual precipitation (MAP) (*15*–*19*) and higher irradiance (*6*, *20*). However, two recent broad-scale surveys of leaf size versus mean annual temperature (MAT) (*18*, *19*) have shown the opposite pattern to that predicted from these daytime energy budget considerations: mean leaf size clearly increases rather than decreases with MAT (*21*). These results pose a substantial challenge to accepted understanding based on "classic" energy budget theory. In other studies, large-leaved species have been shown as uncommon at cold, high-elevation sites (*7*, *22*). This pattern instead accords with control by the nighttime energy balance—an under-appreciated influence—which indicates substantial disadvantage for large leaves in cold regions; they are more prone to frost damage because a thicker boundary layer slows sensible heat exchange with the soil, air, and surrounding vegetation, which is required to offset long-wave radiation losses to the nighttime sky (*23*, *24*).

In this study, our first goal was global-scale quantification of how leaf size varies with site climate, allowing us to analyze the potentially interactive effects of site temperature, irradiance, and moisture and to provide robust tests of predictions from classic optimality-based theories for leaf size (*2*, *9*, *11*–*14*). Our second objective was to model the upper limit to viable leaf sizes in relation to the risks of night-chilling as well as daytime over-heating. By combining analysis of a large worldwide data set with a mechanistic approach to predicting maximum leaf sizes as a function of site climate, we sought to explain the latitudinal gradient in leaf sizes first noted by 19th-century plant geographers (*25*, *26*)—a long-standing ecological conundrum, whose persistence has prevented realistic embedding of this key trait in global vegetation and Earth system models.

We compiled a leaf size data set for 7670 species from 682 nonagricultural sites worldwide, with sampling spread across all vegetated continents, climate zones, biomes, and major growth forms (figs. S1 and S2). At each site, leaf size data were aggregated to a single mean value per species, yielding 13,705 species-site combinations. "Leaf size" here refers to the one-sided projected area of single leaves, leaflets (for compound-leaved species), or leaf analogs (such as phyllodes and cladodes) for otherwise leafless species. Annual and growing-season climate data for each site were derived from source publications or from global climate data sets. Leaf size varied among species by more than five orders of magnitude. On average, trees had larger leaves than shrubs, herbs, or grasses (fig. S2), but very substantial variation could be observed within each growth form. There was also strong taxonomic patterning; for example, families such as Dipterocarpaceae and Magnoliaceae were characterized by many large-leaved species, whereas many small-leaved species were found in Cupressaceae, Ericaceae, and Fabaceae.

Leaf size was on average larger in equatorial regions and smaller toward the poles. A quadratic regression fit to latitude explained 28% of global variation (Fig. 1A), with near-identical trends in simple-leaved and compound-leaved species (fig. S3). Similar or even higher explanatory power was observed within major clades (fig. S4). Common climate metrics associated with latitude explained smaller but still substantial proportions of leaf size variation (Fig. 1 and table S2): MAP (Fig. 1B) and MAT explained 22 and 15% of the global variation, respectively (larger leaves at wetter or warmer sites). Other variables related to site moisture explained less variation than did MAP [such as moisture index (MI), the ratio of annual precipitation to potential evapotranspiration, coefficient of determination (R^2) = 0.12 (Fig. 1C)]. For site temperature, the strongest relationships to leaf size, all positive in sign, were

[1]Department of Biological Sciences, Macquarie University, NSW 2109, Australia. [2]Centre for Past Climate Change and School of Archaeology, Geography and Environmental Sciences (SAGES), University of Reading, Whiteknights, RG6 6AH Reading, UK. [3]Université du Québec à Trois-Rivières, Trois-Rivières, QC G9A 5H7, Canada. [4]AXA Chair in Biosphere and Climate Impacts, Department of Life Sciences, Imperial College London, Silwood Park Campus, Buckhurst Road, Ascot SL5 7PY, UK. [5]Instituto Multidisciplinario de Biología Vegetal (IMBIV), Consejo Nacional de Investigaciones Científicas y Técnicas and Facultad de Ciencias Exactas, Físicas y Naturales, Universidad Nacional de Córdoba, Casilla de Correo 495, 5000 Córdoba, Argentina. [6]Roy M. Huffington Department of Earth Sciences, Southern Methodist University, Dallas, TX 75275, USA. [7]School of Biological Sciences, University of Queensland, St Lucia, QLD 4072, Australia. [8]Institute of Agricultural and Environmental Sciences, Estonian University of Life Sciences, Kreutzwaldi 1, Tartu 51014, Estonia. [9]Department of Forest Resources, University of Minnesota, St. Paul, MN 55108, USA. [10]Hawkesbury Institute for the Environment, Western Sydney University, Penrith 2751, NSW, Australia. [11]Department of Ecology and Evolutionary Biology, University of California, Los Angeles, CA 90095, USA. [12]Área de Ecología, Facultad de Ciencias, Universidad de Córdoba, 14071 Córdoba, Spain. [13]State Key Laboratory of Soil Erosion and Dryland Farming on the Loess Plateau, College of Forestry, Northwest A & F University, Yangling 712100, China. [14]Department of Geosciences, Pennsylvania State University, University Park, PA 16802, USA.
*Corresponding author. Email: ian.wright@mq.edu.au

with climate variables expressed on a growing season basis [mean growing season temperature, R^2 = 0.21 (Fig. 1D); mean temperature of the coldest month during the growing season, R^2 = 0.24]. Leaf size was statistically correlated with irradiance, but with little explanatory power (R^2 < 0.01, P = 0.002) (Fig. 1E). In general, relationships between leaf size and individual climate variables were tighter in woody than in nonwoody species and, among woody taxa, tighter in evergreen than in deciduous species (tables S3 and S4).

Combinations of climate variables explained the most variation in leaf size. Site temperature [most notably, mean temperature during the warmest month (T_{WM})], irradiance, and moisture (MAP or MI) showed strong interactive effects, with best-fit surfaces being twisted planes (Fig. 2 and fig. S5). At the driest sites (MAP < ~800 mm or MI < ~0.5), leaf size weakly decreased with T_{WM}, whereas across wetter sites, leaf size increased with T_{WM} (R^2 = 0.34) (Fig. 2). This coupling with site temperature was increasingly steep and tight at higher MAP (fig. S6A). Similarly, leaf size was unrelated to MAP at colder sites (T_{WM} in the range from 0° to 15°C) but was positively related to MAP at warmer sites, and increasingly so the higher the T_{WM} (fig. S6C). Qualitatively similar patterns with similar explanatory power were found when substituting irradiance for T_{WM} in these analyses (figs. S5 and S6, B and D), or MI for MAP (R^2 = 0.33): Leaves were smaller at drier sites only in warm regions, smaller at hotter or higher irradiance sites only in dry regions, and smaller at colder sites, especially under wetter conditions. That is, each of the individual predictions from previous leaf energy balance theory was supported under specific conditions, but none was universally true.

Our empirical analyses indicated that the upper limits to leaf size showed marked trends both with latitude (quantile regression slopes in Fig. 1A and fig. S4) and climate (fig. S6, A to D; quantile regressions in Fig. 1, B to D, and fig. S5; and table S2). To explore this upper-limit issue more deeply, we developed a simple but robust approach to energy-balance modeling for both daytime and nighttime leaf-to-air temperature differences (fig. S8). Energy balance theory (*2*, *4*) predicts that the net radiation at the leaf surface in steady state must be equal to the sum of sensible and latent heat exchanges with the surrounding air, the former being proportional to the leaf-to-air temperature difference (ΔT), the latter to the transpiration rate. On the basis of this theory, we applied a generic calculation to predict upper bounds on leaf size during the daytime, for each study site. We assumed that plants cannot transpire faster than at the maximum rate allowed by the net radiation balance of the leaf and the temperature of the air, and that the transpiration rate is progressively reduced as soil moisture availability declines. Using the well-established relationship between leaf boundary-layer conductance (g_b) and size (*4*, *9*), we can then derive for any given set of climatic conditions the maximum leaf size that keeps leaf temperature below a specified upper limit throughout the year.

We also considered the energy balance of leaves during the nighttime, when net radiation is negative and the extent to which this is compensated by sensible heat exchange determines ΔT (*23*, *24*). For this calculation of maximum expected leaf size, we specified a lower temperature limit below which active leaves would be expected to suffer serious damage. We considered

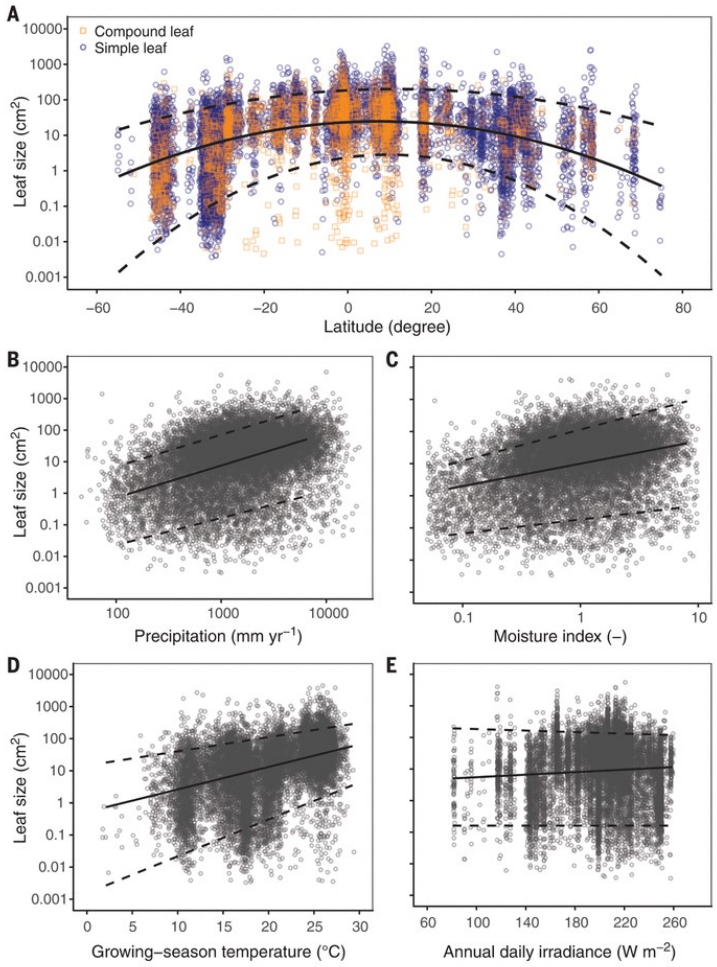

Fig. 1. Global trends in leaf size (LS) in relation to latitude and climate. (**A**) Species are coded as simple-leaved (blue circles) or compound-leaved (orange squares; for which "leaf size" refers to that of the leaflets). Solid fitted line (quadratic regression, all species), logLS = 1.37 + 0.006 Lat − 0.0004 Lat^2; R^2 = 0.28, P < 0.0001. Shown in fig. S3, A and B, are equivalent graphs, with slopes fitted separately to simple- and compound-leaved species, and when considering leaf size of compound leaves to be that of the entire leaf rather than that of the leaflets. (**B**) Mean annual precipitation (logLS = 1.02 logMAP − 2.18; R^2 = 0.22, P < 0.0001). (**C**) Annual equilibrium MI (logLS = 0.70 logMI + 1.00; R^2 = 0.12, P < 0.0001). (**D**) Mean temperature during the growing season (logLS = 0.07 T_{gs} − 0.28; R^2 = 0.21, P < 0.0001). (**E**) Annual daily radiation (logLS = 0.002 RAD + 0.54; R^2 = 0.002, P = 0.002). In (A) to (E), fitted slopes were estimated by using linear mixed models (site and species treated as random effects); further details of leaf size–climate relationships are given in table S2. In (A) to (E), sample n = 13,641 species-site combinations and dashed lines show the 5th and 95th quantile regression fits. Further analysis by using quantile regression is presented in fig. S7.

only temperatures encountered during the thermal growing season, on the basis that leaves in the coldest part of the year in cold-winter climates will be shed or cold-hardened and dormant. On the basis of these two constraints—applying an upper leaf temperature limit of 50°C (*27*, *28*), and a lower temperature limit of −5°C (*29*)—we derived two predictions of maximum viable leaf size for each of the 682 sites in our data set. From these data, we derived general predictions for latitudinal trends in maximum leaf size and compared them with observed data (Fig. 3 and figs. S9 to S12).

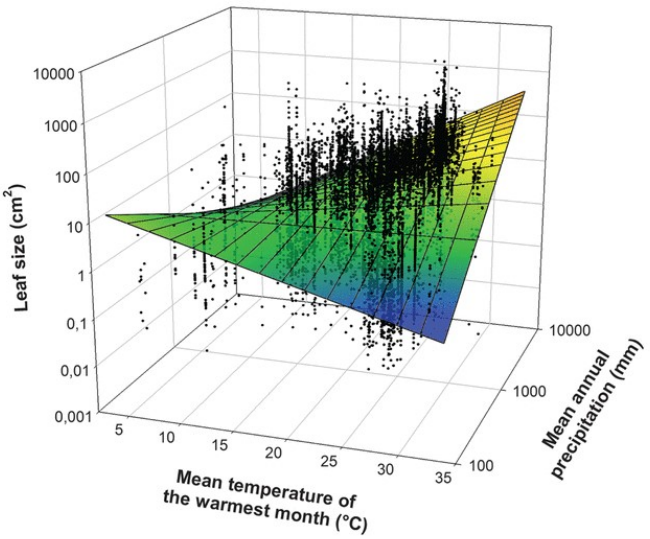

Fig. 2. Global variation in leaf size as a function of site temperature and precipitation. Considering leaf size (LS) as a function of mean temperature of the warmest month (T_{WM}) and mean annual precipitation (MAP), the best-fit surface estimated by multiple mixed-model regression was a twisted plane with the form logLS = − 0.27 T_{WM} − 1.32 logMAP + 0.10 T_{WM} × logMAP + 4.01 (all parameters P = 0.001; R^2 = 0.34; n = 13,641 species-site combinations). Similar results were found in analyses involving irradiance rather than T_{WM}, or annual moisture index (MI) rather than precipitation (figs. S5 and S6).

At arid sites (MI < 0.5) (Fig. 3A), the upper boundary of leaf size is almost universally consistent with estimated daytime constraints (Fig. 3, red dashed line) because rapid transpiration is impossible when water supply is limited, and large leaves are disadvantaged by reaching damagingly high temperatures. At intermediate-MI sites (Fig. 3B), daytime constraints appear more limiting between ~20° S and 20° N, but nighttime constraints dominate outside this zone. At wet sites (MI > 1.5) (Fig. 3C), daytime constraints are predicted to be unimportant because sufficient water is generally available for effective transpirational cooling, with nighttime constraints dominating at all latitudes.

These results can be generalized in the form of global maps showing geographic trends in maximum leaf size (Fig. 4) and its determinants (fig. S13). Maximum viable leaf sizes are shown to be especially small both in warm deserts and cold, high-elevation regions (such as Tibet and the Andes), but for different reasons relating to daytime and nighttime constraints, respectively. Steep gradients of predicted maximum leaf size can be found, for example, where arid subtropics transition into wet tropics. In very warm (day and night), ever-wet climates, there may be no effective thermal constraint on leaf size (figs. S4, deep blue shade, and S13, "unlimited" category). In these situations, it is likely that other limits to leaf size come into play, such as the biomechanics of support (*6*) or whole-plant hydraulic architecture (*30*). We estimate that these situations represent 4.3%

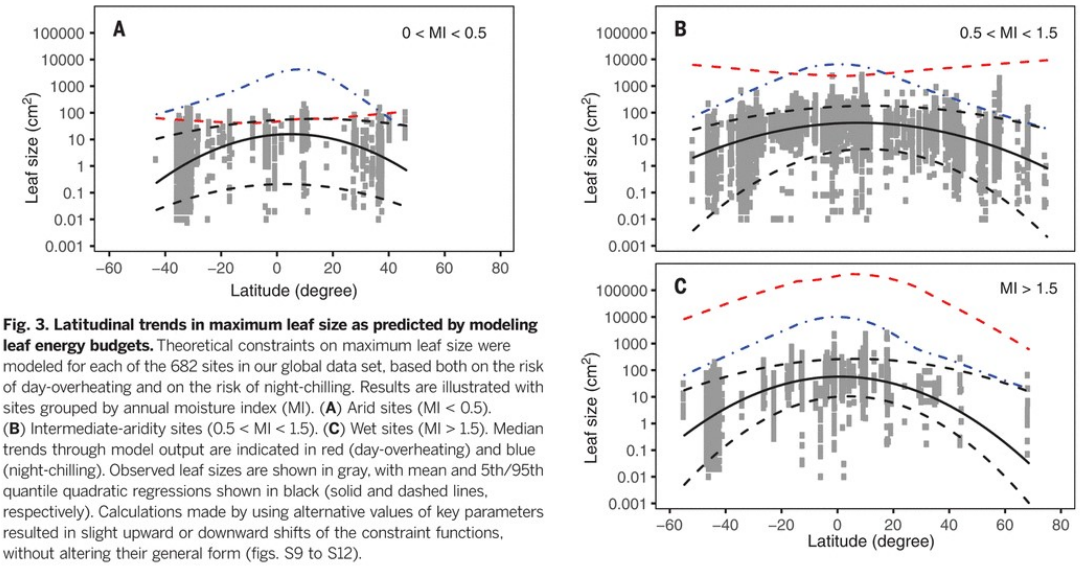

Fig. 3. Latitudinal trends in maximum leaf size as predicted by modeling leaf energy budgets. Theoretical constraints on maximum leaf size were modeled for each of the 682 sites in our global data set, based both on the risk of day-overheating and on the risk of night-chilling. Results are illustrated with sites grouped by annual moisture index (MI). (**A**) Arid sites (MI < 0.5). (**B**) Intermediate-aridity sites (0.5 < MI < 1.5). (**C**) Wet sites (MI > 1.5). Median trends through model output are indicated in red (day-overheating) and blue (night-chilling). Observed leaf sizes are shown in gray, with mean and 5th/95th quantile quadratic regressions shown in black (solid and dashed lines, respectively). Calculations made by using alternative values of key parameters resulted in slight upward or downward shifts of the constraint functions, without altering their general form (figs. S9 to S12).

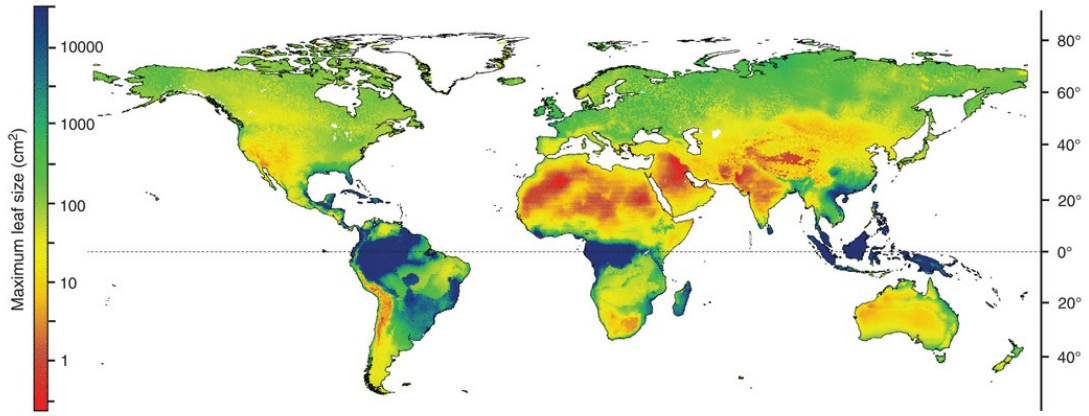

Fig. 4. Predicted geographic trends in maximum leaf size. Each grid cell is color coded according to the smaller of the two predictions for maximum leaf size (daytime or nighttime) (fig. S13), made by using the same procedure as the site-specific modeling. Areas coded the deepest shade of blue are those where there may be no effective thermal constraint on maximum leaf size because sufficient water is generally available for effective transpirational cooling, and warm nighttime air temperatures prevent leaves from suffering radiative frost damage.

of global land area, whereas nighttime constraints provide the dominant control for 51%, daytime constraints 38%, and night and day constraints colimit leaf sizes for 6.7% of land (fig. S13).

Our model is based on a first-order empirical approximation to transpiration that can be derived in terms of boundary-layer theory (*31*, *32*). It is likely to be more accurate for canopy species. All else being equal, lower energy inputs in shaded situations may allow for larger leaf sizes than predicted (*6*, *11*–*13*, *33*), whereas shallow-rooted species with restricted access to water might have smaller leaf sizes than predicted (*34*). More explicit modeling of leaf-level energy balance is possible. However, consideration of, for example, vertical gradients of leaf size would also entail modeling of within-canopy humidity and wind speeds, which is a more complex task.

What are the selective advantages that favor large leaves under conditions when they are physiologically possible? This is not well understood, but two prospective explanations seem most promising. First, by deploying a given leaf mass as fewer, larger leaves, the associated twig costs tend to be lower (*13*, *35*), even if within-leaf structural costs are higher (*36*). All else being equal, this should lead to a growth advantage (*37*). Second, the wider leaf-to-air temperature differences possible for larger leaves may allow them to more quickly heat up to favorable temperatures for photosynthesis during cool mornings, leading to substantially higher photosynthetic returns (*5*). In addition, under sufficiently hot and high-irradiance conditions, wider leaf-to-air temperature differences may allow larger leaves to operate at temperatures substantially lower than that of the surrounding air (and more favorable for photosynthesis), provided sufficient soil water is available to support the necessary transpiration (*9*, *38*, *39*).

A wide range of leaf sizes exists at any given climate or latitude (Fig. 1). Leaf size is coordinated with many other features of plant architecture, canopy display, and plant hydraulics (*6*, *7*, *13*, *30*, *35*, *40*), apparently leading to many equally viable leaf size strategies for a given climate. Additional factors are known to influence leaf size; most notably, low-nutrient soils are characterized by smaller-leaved species (*6*, *17*), smaller-leaved species seemingly suffer less herbivory (*41*), and as already noted, larger leaves may be favored under deep shade (*6*, *11*–*13*, *33*). Nonetheless, it appears that climate provides the dominant control on the global geographic limits to leaf size, acting both through daytime and nighttime constraints. The nighttime constraint on leaf size in seasonally cold climates has featured in literature on alpine regions and on frost risks in agriculture (*23*, *24*), but its generality has not previously been noted.

Our analyses have moved beyond consideration of bivariate leaf size–climate relationships (*6*, *7*, *15*–*22*), and in doing so, they show simple, interpretable patterns that had not emerged from previous analyses of more limited sets of observations. By pairing broad-scale data synthesis with a simple and robust approach to leaf energy balance modeling, we have shown that the key to understanding geographical limits to leaf size is the leaf-to-air temperature difference, which reflects the balance of energy inputs and outputs. This approach provides a quantitative explanation for the latitudinal gradient in leaf size, one of the oldest observations in ecology (*25*, *26*), for which no general theory existed previously. This knowledge has the potential to enrich "next-generation" vegetation models, in which leaf temperature and water use during photosynthesis play key roles, and to constrain predictions from species distribution models in relation to climate change. It will aid reconstruction of paleoclimate from leaf macrofossils (*15*, *16*, *19*, *21*), an enterprise that also dates back more than a century (*42*) but which, until now, has relied entirely on empirical relationships between leaf traits and climate.

REFERENCES AND NOTES

1. H. G. Jones, *Plants and Microclimate: A Quantitative Approach to Environmental Plant Physiology* (Cambridge Univ. Press, ed. 3, 2014).
2. D. M. Gates, *Ecology* **46**, 1–13 (1965).
3. W. Larcher, *Physiological Plant Ecology. Ecophysiology and Stress Ecology of Functional Groups* (Springer-Verlag, ed. 4, 2003).
4. G. S. Campbell, J. M. Norman, *An Introduction to Environmental Biophysics* (Springer, ed. 2, 1998).
5. S. T. Michaletz *et al.*, *Nat. Plants* **2**, 16129 (2016).
6. T. J. Givnish, *New Phytol.* **106** (suppl.), 131–160 (1987).
7. C. Körner, M. Neumayer, S. P. Menendez-Riedl, A. Smeets-Scheel, *Flora* **182**, 353–383 (1989).
8. S. Díaz *et al.*, *Nature* **529**, 167–171 (2016).
9. D. M. Gates, *Annu. Rev. Plant Physiol.* **19**, 211–238 (1968).
10. A. Leigh, S. Sevanto, J. D. Close, A. B. Nicotra, *Plant Cell Environ.* **40**, 237–248 (2017).
11. D. F. Parkhurst, O. L. Loucks, *J. Ecol.* **60**, 505–537 (1972).
12. T. J. Givnish, G. J. Vermeij, *Am. Nat.* **110**, 743–778 (1976).
13. T. J. Givnish, in *Physiological Ecology of Plants of the Wet Tropics*, E. Medina, H. A. Mooney, C. Vázquez-Yánes, Eds. (Dr W Junk Publishers, 1984), pp. 51–84.
14. S. E. Taylor, in *Perspectives of Biophysical Ecology*, D. M. Gates, R. B. Schmerl, Eds. (Springer-Verlag, 1975), pp. 73–86.
15. B. F. Jacobs, *Palaeogeogr. Palaeoclimatol. Palaeoecol.* **145**, 231–250 (1999).
16. P. Wilf, S. L. Wing, D. R. Greenwood, C. L. Greenwood, *Geology* **26**, 203–206 (1998).
17. C. R. Fonseca, J. M. Overton, B. Collins, M. Westoby, *J. Ecol.* **88**, 964–977 (2000).
18. A. T. Moles *et al.*, *J. Veg. Sci.* **25**, 1167–1180 (2014).
19. D. J. Peppe *et al.*, *New Phytol.* **190**, 724–739 (2011).
20. D. Ackerly, C. Knight, S. Weiss, K. Barton, K. Starmer, *Oecologia* **130**, 449–457 (2002).
21. D. R. Greenwood, *Rev. Palaeobot. Palynol.* **71**, 149–190 (1992).
22. S. R. P. Halloy, A. F. Mark, *J. R. Soc. N. Z.* **26**, 41–78 (1996).

23. R. Leuning, *Agric. Meteorol.* **42**, 135–155 (1988).
24. D. N. Jordan, W. K. Smith, *Agric. Meteorol.* **71**, 359–372 (1994).
25. A. F. W. Schimper, *Plant Geography Upon a Physiological Basis* (Clarendon Press, 1903).
26. E. Warming, *Oecology of Plants* (Clarendon Press, 1909).
27. E. M. Curtis, C. A. Knight, K. Petrou, A. Leigh, *Oecologia* **175**, 1051–1061 (2014).
28. Z. H. Hu, Y. N. Xu, Y. D. Gong, T. Y. Kuang, *Photosynthetica* **43**, 529–534 (2005).
29. Y. Vitasse, A. Lenz, G. Hoch, C. Körner, *J. Ecol.* **102**, 981–988 (2014).
30. K. H. Jensen, M. A. Zwieniecki, *Phys. Rev. Lett.* **110**, 018104 (2013).
31. M. R. Raupach, *Q. J. R. Meteorol. Soc.* **127**, 1149–1181 (2001).
32. C. Huntingford, J. L. Monteith, *Boundary-Layer Meteorol.* **88**, 87–101 (1998).
33. N. Chiariello, in *Physiological Ecology of Plants of the Wet Tropics*, E. Medina, H. A. Mooney, C. Vázquez-Yánes, Eds. (Dr W Junk Publishers, 1984), pp. 85–98.
34. D. D. Ackerly, *Ecol. Monogr.* **74**, 25–44 (2004).
35. I. J. Wright, D. S. Falster, M. Pickup, M. Westoby, *Physiol. Plant.* **127**, 445–456 (2006).
36. U. Niinemets *et al.*, *Ann. Bot.* **100**, 283–303 (2007).
37. M. Pickup, M. Westoby, A. Basden, *Funct. Ecol.* **19**, 88–97 (2005).
38. W. K. Smith, *Science* **201**, 614–616 (1978).
39. N. Dong, I. C. Prentice, S. P. Harrison, Q. H. Song, Y. P. Zhang, *Glob. Ecol. Biogeogr.* **26**, 998–1007 (2017).
40. L. Sack *et al.*, *Nat. Commun.* **3**, 837 (2012).
41. A. T. Moles, M. Westoby, *Oikos* **90**, 517–524 (2000).
42. I. W. Bailey, E. W. Sinnott, *Science* **41**, 831–834 (1915).

ACKNOWLEDGMENTS

We thank the following people who generously provided access to previously unpublished trait data or data otherwise unavailable from source publications: D. Ackerly, H. Cornelissen, W. Cornwell, D. Duncan, E. Garnier, L. Yulin, J. Lloyd, H. Morgan, T. Navarro, J. Oleksyn, J. Overton, O. Phillips, N. Pitman, H. Poorter, L. Poorter, C. Vriesendorp, J. Wright, and A. Zanne. J. Cooke, T. Lenz, A. Ordonez, and J. Suitch helped compile and error-check trait data. This research was funded by the Australian Research Council (grants RN0459908, DP0558411, and FT100100910) and by Macquarie University (Ph.D. scholarship supporting N.D.) and is a contribution to the AXA Chair Programme in Biosphere and Climate Impacts and the Imperial College initiative on Grand Challenges in Ecosystems and the Environment. R.V. was funded by the Spanish Ministerio de Educación y Ciencia project ECO-MEDIT (CGL2014-53236-R) and European Fondo Europeo de Desarrollo Regional funds. B.F.J. acknowledges support from the National Science Foundation (USA), grant EAR-9510015. This work originated from a working group held at Macquarie University. The leaf trait data set was compiled by I.J.W., E.A.L., and R.V.G., from literature data and data provided by S.D., R.V.G., B.F.J., R.K., M.R.L., Ü.N., P.B.R., R.V., M.W., P.W., and I.J.W. Geographic and climate data were compiled or calculated by I.J.W., E.A.L., V.M., and H.W. Statistical analyses were run by V.M. and I.J.W. The modeling component was conceived by I.C.P., N.D., and I.J.W. and run by N.D. L.S. initially suggested teaming empirical analysis with energy balance models. V.M., N.D., and R.V. created the figures. I.J.W. drafted the initial manuscript with assistance from I.C.P. All coauthors contributed to subsequent versions. The "global leaf size data set" is available as an Excel workbook in the supplementary materials.

SUPPLEMENTARY MATERIALS

www.sciencemag.org/content/357/6354/917/suppl/DC1
Materials and Methods
Figs. S1 to S13
Tables S1 to S4
References (*43*–*181*)
Data Set S1

26 November 2016; accepted 2 August 2017
10.1126/science.aal4760

TRANSCRIPTION

Structure of the complete elongation complex of RNA polymerase II with basal factors

Haruhiko Ehara,[1] Takeshi Yokoyama,[1] Hideki Shigematsu,[1] Shigeyuki Yokoyama,[2] Mikako Shirouzu,[1] Shun-ichi Sekine[1]*

In the early stage of transcription, eukaryotic RNA polymerase II (Pol II) exchanges initiation factors with elongation factors to form an elongation complex for processive transcription. Here we report the structure of the Pol II elongation complex bound with the basal elongation factors Spt4/5, Elf1, and TFIIS. Spt4/5 (the Spt4/Spt5 complex) and Elf1 modify a wide area of the Pol II surface. Elf1 bridges the Pol II central cleft, completing a "DNA entry tunnel" for downstream DNA. Spt4 and the Spt5 NGN and KOW1 domains encircle the upstream DNA, constituting a "DNA exit tunnel." The Spt5 KOW4 and KOW5 domains augment the "RNA exit tunnel," directing the exiting nascent RNA. Thus, the elongation complex establishes a completely different transcription and regulation platform from that of the initiation complexes.

Transcription is accomplished by DNA-dependent RNA polymerase (RNAP) through a multistep process consisting of initiation, elongation, and termination. In the initiation of eukaryotic mRNA transcription, RNA polymerase II (Pol II) is associated with general transcription factors (GTFs), forming a huge initiation complex (IC) on the DNA (*1*–*3*). After the synthesis of a certain length of RNA, the GTFs are replaced with elongation factors (EFs). Thus, the IC isomerizes into a processive elongation complex (EC), which serves as a platform for regulation and various transcription-coupled events, such as mRNA processing, chromatin remodeling, and DNA repair (*4*–*7*). Although recent advances in cryo–electron microscopy (cryo-EM) have revealed several IC structures (*1*–*3*), the architecture of the EC still remained elusive. Here we elucidated the Pol II EC structure, including the conserved basal EFs Spt4/5, Elf1, and TFIIS, by using an integrated approach combining x-ray crystallography and cryo-EM.

[1]RIKEN Center for Life Science Technologies, 1-7-22 Suehiro-cho, Tsurumi-ku, Yokohama 230-0045, Japan. [2]RIKEN Structural Biology Laboratory, 1-7-22 Suehiro-cho, Tsurumi-ku, Yokohama 230-0045, Japan.
*Corresponding author. Email: shunichi.sekine@riken.jp

Spt4/5, a heterodimeric complex of Spt4 and Spt5 (NusG in bacteria), is implicated in processive transcription elongation (*8*, *9*), promoter-proximal pausing in higher eukaryotes (as DRB sensitivity-inducing factor) (*8*, *10*), and many transcription-coupled events (*4*–*7*). Spt5 is a multidomain protein composed of the conserved NGN (NusG N-terminal) domain, which binds Spt4, and different numbers of KOW (Kyprides-Onzonis-Woese) domains, which are connected by flexible linkers and the C-terminal repeat region (CTR) (Fig. 1A) (*11*–*13*). Multiple KOW domains specific to eukaryotic Spt5 are crucial for the establishment of the EC and Spt4/5 functions (*14*, *15*), but their locations on Pol II and functions in transcription have remained enigmatic. To assess which KOW domain is essential for Pol II binding and transcription, we created a series of Spt4/5 variants and investigated their transcription-stimulation functions for Pol II from the yeast *Komagataella pastoris* (*16*) (Fig. 1, A and B). Surprisingly, only KOW5 is necessary and sufficient for the transcription stimulation, whereas the other KOW domains, the NGN domain, and Spt4 were dispensable. These data underscore the importance of KOW5 in the Spt4/5 function as an EF.

Elongation factor 1 (Elf1 in yeast; ELOF1 in human) is a small protein conserved in eukaryotes and several archaeal classes, including Crenarchaeota (fig. S1) (*17*). Elf1 displays synthetic lethality with several EFs, including Spt4, Spt5, and TFIIS in yeast (*18*). Chromatin immunoprecipitation analyses revealed that Elf1 accompanies transcribing Pol II in vivo (*18*, *19*). As Elf1 slightly delays transcription elongation by *K. pastoris* Pol II in vitro, it seems to directly interact with Pol II and function in transcription regulation (fig. S2).

To understand how the Spt5 KOW5 domain and Elf1 associate with Pol II, we solved the cocrystal structure of the *K. pastoris* Pol II EC